JOURNAL OF SPACECRAFT AND ROCKETS
Vol. 38, No. 3, May–June 2001

Heat Transfer Through Cryogenic Propellant Tank Insulation During Ground-Hold Conditions

T. K. Nandi*
Birla Institute of Technology, Ranchi 835 215, India

A theoretical formulation is presented for predicting transient (leading to steady state) heat-transfer characteristics through the thermal insulation of cryogenic rocket propellant tanks. Only the cylindrical sides of the propellant tanks are studied while the rocket is on the launch pad in a holding condition. Effects of direct solar radiation, Earth-reflected/emitted radiation, and wind velocity are considered for estimation of heat loads to the propellants. A finite difference technique using a simple explicit method is adopted to establish time-dependent temperature distributions across several layers of the integrated insulation package. Stability, accuracy, and computational requirements of the technique are reviewed with simple implicit and Crank–Nicolson solution schemes. Computed results are compared with Galerkin finite element solutions using linear and quadratic polynomial interpolants. Formulations for these finite element methods are also derived. The model can be used for characterizing insulation material, thickness optimization, estimation of boil-off rate, and verification of lower limit temperature at the outer surface. Some results based on relevant input data are presented.

Nomenclature

A	=	surface area, m^2
Cp	=	specific heat at constant pressure, J/kg-K
d	=	number of days from 1 January to the launch date
F_{SE}	=	radiation shape factor from vertical tank surface to the Earth horizontal surface
h	=	convection heat-transfer coefficient, W/m^2-K
I_D	=	intensity of direct solar radiation per unit area on Earth surface, W/m^2
k	=	thermal conductivity, W/m-K
Nu	=	Nusselt number
Pr	=	Prandtl number
$\dot{Q}_{COND}$	=	conduction heat transfer, W
$\dot{q}_{CONV}$	=	convection heat transfer from environment to insulation surface, W/m^2
$\dot{q}_{RADI}$	=	incident radiation on insulation surface, W/m^2
$\dot{q}_{RADO}$	=	radiation heat transfer from insulation surface to atmospheric air, W/m^2
$\dot{q}_{SD}$	=	direct solar radiation, W/m^2
$\dot{q}_{SE}$	=	Earth-emitted radiation, W/m^2
$\dot{q}_{SR}$	=	Earth-reflected radiation, W/m^2
Re	=	Reynolds number
S	=	solar constant, W/m^2
T	=	temperature, K
t	=	time, s
x	=	distance, m
y	=	factor for turbidity of air
z	=	relative thickness of air mass
α	=	tilt angle between Earth and the surface, deg
β	=	thermal diffusivity, m^2/s
γ	=	azimuth angle of the surface (due south = 0, east+, west−), deg
ΔT	=	temperature difference, K
Δt	=	time interval, s
Δx	=	layer thickness, m
ε	=	emissivity at low temperature
ε'	=	emissivity for solar radiation
ζ	=	angle between the sun's ray and the equatorial plane at solar noon (north+, south−), deg
θ	=	angle between sun rays and normal to the surface, deg
ρ	=	density, kg/m^3
σ	=	Stefan–Boltzmann constant, W/m^2-K^4
ϕ	=	latitude angle of the launch site (equator = 0, north+, south−), deg
ω	=	hour angle (solar noon = 0, morning+, afternoon−), deg

Subscripts

e	=	Earth surface
i	=	ith layer
j	=	jth node
$j, j \pm n$	=	from jth node to $(j \pm n)$th node (n is an integer)
s	=	insulation surface
0	=	tank wall
∞	=	atmospheric

Introduction

CRYOGENIC propellants in rocket stage tanks are thermally protected with an insulation package to minimize boil-off losses, propellant heating, tank pressure rise, and thermal stratification. With weight being the major design constraint, foam type materials, which do not require a double-wall housing with a vacuum layer, are the most commonly used insulation for such applications.[1–3] Other than foam materials, primer, adhesives, heat shielding coatings, etc. are used as the supportive layers for the insulation package. An appropriate model for computing heat in-leak is essential for thermal design of such an integrated insulation system.

In this article theoretical formulations are presented for estimating transient heat transfer through the thermal insulation of cryogenic propellant tanks. Only the cylindrical sides of the propellant tanks are considered. The proposed model considers the heat fluxes on the outer surface as a result of direct solar radiation, Earth-reflected/emitted radiation, and wind velocity. A finite difference technique using the simple explicit method is adopted to establish time-dependent temperature profiles in the integrated insulation package. Stability, accuracy, and computational details of the technique are reviewed with simple implicit and Crank–Nicolson solution methods. A comparison is also presented with results obtained by Galerkin finite element methods. Results based on relevant input data are presented.

Assumptions

The following assumptions have been made for establishing transient temperature profiles and predicting heat in-leak to the cryogenic propellants: 1) heat transfer is only in the radial direction; 2) at

Received 10 August 2000; revision received 30 October 2000; accepted for publication 1 November 2000.

*Associate Professor, Department of Space Engineering and Rocketry.

$t = 0$ all of the insulating materials are assumed to have the same temperature as that of the surface, and the tank wall temperature is equal to the propellant temperature; 3) changes of propellant temperature and the tank wall temperature (as a result of the change of tank pressure and heat in-leak) are assumed to have little effect on the rate of heat in-leak and hence are neglected; and 4) effect of ice formation on insulation surface is neglected.

Surface Temperature at $t = 0$

The surface temperature at $t = 0$, T_S, is computed from the thermal equilibrium conditions with the surrounding atmosphere. Heat fluxes that are encountered between the tank's insulation surface and the surroundings are 1) incident solar radiation and Earth-emitted/ reflected radiation $\dot{q}_{\text{RADI}}$, 2) radiation heat exchange with the surrounding air $\dot{q}_{\text{RADO}}$, and 3) convection heat transfer caused by wind velocity $\dot{q}_{\text{CONV}}$. Under thermal equilibrium condition the heat balance equation can be expressed as

$$\dot{q}_{\text{RADI}} + \dot{q}_{\text{RADO}} + \dot{q}_{\text{CONV}} = 0 \tag{1}$$

Incident Solar Radiation and Earth-Emitted/Reflected Radiation $\dot{q}_{\text{RADI}}$

Total heat flux caused by direct solar radiation, Earth-emitted radiation, and Earth-reflected radiation that are absorbed by a unit area of the insulation surface is estimated from

$$\dot{q}_{\text{RADI}} = \varepsilon'_S(\dot{q}_{\text{SD}} + F_{\text{SE}}\dot{q}_{\text{SR}}) + \varepsilon_S F_{\text{SE}}\dot{q}_{\text{SE}} \tag{2}$$

Incident Solar Radiation $\dot{q}_{\text{SD}}$

Direct solar energy per unit area of any surface on Earth can be computed from the relation[4,5]

$$\dot{q}_{\text{SD}} = I_D \cos\theta \tag{3}$$

Intensity of direct solar radiation I_D is dependent on the solar constant S, relative thickness of the air mass z, and turbidity of air factor y. A simple formula for estimating I_D is given by[4]

$$I_D = S \exp(-y a_{\text{ms}} z) \tag{4}$$

where $z = \sec\theta_e$, $a_{\text{ms}} = 0.128 - 0.054 \log z$, and θ_e is the angle of incidence on Earth's horizontal surface. The turbidity factor y varies from two for very clear sky to four or five for a smoggy, industrial environment.

The angle of incidence θ for any surface on Earth is conveniently defined by[5]

$$\cos\theta = a \sin\zeta + b \cos\zeta \cos\omega + c \cos\zeta \sin\omega \tag{5}$$

where

$$a = \sin\phi \cos\alpha - \cos\phi \sin\alpha \cos\gamma \tag{6}$$

$$b = \cos\phi \cos\alpha + \sin\phi \sin\alpha \cos\gamma \tag{7}$$

$$c = \sin\alpha \sin\gamma \tag{8}$$

$$\zeta = 23.45 \sin\left(360\frac{284 + d}{365}\right) \text{deg} \tag{9}$$

To consider the angular variation of solar radiation, the cylindrical surfaces of the vertical tanks are divided into 12 equal sections in which section-I, section-IV, section-VII and section-X face due south, due east, due north, and due west, respectively, as shown in Fig. 1. Only the value of orientation angle γ, in Eqs. (6–8), will change while computing incidence ($\cos\theta$) for different sections. A negative value of $\cos\theta$ would indicate no direct solar energy on the surface.

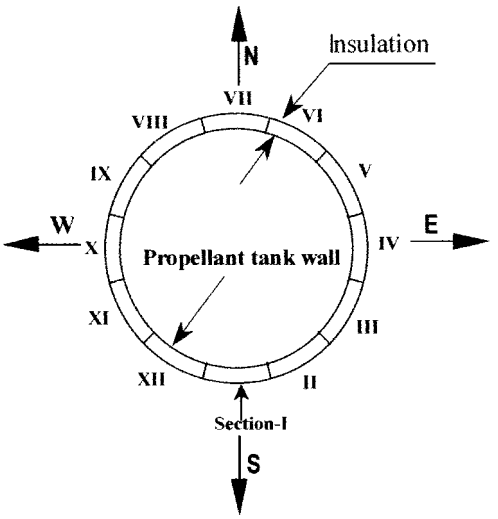

Fig. 1 Division of tank insulation.

Earth-Reflected Radiation $\dot{q}_{\text{SR}}$

Earth-reflected solar radiation is estimated from

$$\dot{q}_{\text{SR}} = \text{albedo} \times I_D \times \cos\theta_e \tag{10}$$

$$\cos\theta_e = \sin\phi \sin\zeta + \cos\phi \cos\zeta \cos\omega \tag{11}$$

The term *albedo* is the fraction of incident energy that is reflected. The equation for $\cos\theta_e$ is obtained by setting $\alpha = 0$ (for horizontal surface) in Eqs. (6–8) to obtain $a = \sin\phi$, $b = \cos\phi$, and $c = 0$, which in turn are used in Eq. (5) to obtain Eq. (11). The value for I_D is obtained from Eq. (4).

Earth-Emitted Radiation $\dot{q}_{\text{SE}}$

Energy that radiates from the Earth surface as a result of its own temperature can be computed from the relation

$$\dot{q}_{\text{SE}} = \varepsilon_e \sigma T_e^4 \tag{12}$$

Earth temperature T_e can be obtained from the equilibrium temperature of the Earth considering incident solar radiation, energy radiation caused by Earth's own temperature, and convective heat transfer from the Earth's surface to the surrounding air. The equation is expressed as

$$\varepsilon'_e I_D \cos\theta_e = \varepsilon_e \sigma\left(T_e^4 - T_\infty^4\right) + h(T_e - T_\infty) \tag{13}$$

The convective heat-transfer coefficient h is dependent on the air velocity. The correlation[4] $h = 1.52(\Delta T)^{1/3}$ for turbulent natural convection from hot plate facing upward could be used for a simple estimation. Equation (13) is solved for T_e iteratively.

Radiation Shape Factor F_{SE}

The geometry for computing the shape factor between vertical tank surface and the horizontal Earth surface is shown in Fig. 2. The shape factor between any differential element on vertical surface (dA_1) and a strip element on the infinite horizontal surface is[6]

$$dF_{d1-2} = \tfrac{1}{2} d(\sin\psi) \tag{14}$$

Integrating over the part of the infinite surface visible to the element dA_1,

$$F_{d1-2} = \int_0^{\pi/2} \frac{1}{2} d(\sin\psi) = \frac{1}{2} \tag{15}$$

Because this applies to every element on the cylindrical surface, it follows that the fraction from the entire cylinder to the infinite horizontal plane is the same, and so $F_{\text{SE}} = F_{1-2} = 0.5$.

Table 1 Constant and power indices for average heat transfer to a cylinder in crossflow[7]

Region (deg from stagnation point)	u	v	w
0–90/105	0.32	0.6	0.33
90/105–120/135	0.03	0.9	0.45
120/135–180	0.02	0.85	0.45

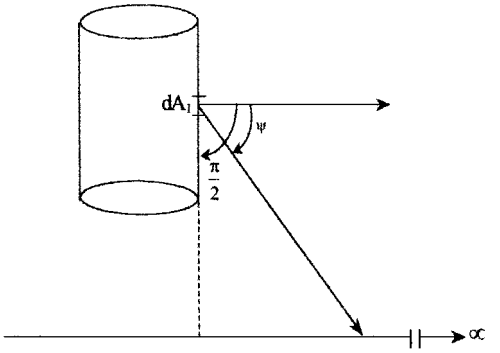

Fig. 2 Geometry for vertical cylindrical surface placed over an infinite horizontal surface for computing radiation shape factor.

Radiation Heat Exchange with the Surrounding Air $\dot{q}_{\mathrm{RADO}}$

Radiation heat exchange between the tank surface and the surrounding atmospheric air can be estimated from (shape factor = 1)

$$\dot{q}_{\mathrm{RADO}} = \varepsilon_s \sigma \left(T_\infty^4 - T_S^4\right) \tag{16}$$

Convection Heat Transfer Caused by Wind Velocity $\dot{q}_{\mathrm{CONV}}$

For zero wind velocity a standard free-convection correlation[4] for a vertical surface is used. In the presence of wind, a forced-convection correlation[7] for crossflow over a cylinder is used for computing the Nusselt number. Convection heat transfer per unit area is estimated from

$$\dot{q}_{\mathrm{CONV}} = h(T_\infty - T_S) \tag{17}$$

A general equation for Nusselt number is used: $Nu = u\,Re^v Pr^w$, with specific values of u, v, and w defined in Table 1. The angular position 0 in Table 1 indicates the forward stagnation point. The other two positions 90 to 105 and 120 to 135 correspond to laminar-to-turbulent transition and separation points, respectively.

To solve Eq. (1) and to obtain surface temperature at $t = 0$, we need the value of T_S in Eqs. (16) and (17). Therefore the solution is obtained in an iterative manner starting with an assumption of surface temperature T_S.

Transient Temperature Profile

A design of an integrated insulation package comprising foam as the main insulating material and other supportive layers is shown in Fig. 3. The total number of layers n are identified in the following manner: layer 1 = primer coating, layer 2 = adhesive coating, layer 3 to layer $n-3$ = foam insulation, layer $n-2$ = second adhesive coating, layer $n-1$ = ablative layer, and layer n = antistatic coating. This layering is illustrated in Fig. 4.

From the heat balance relationship, the heat equivalent to the rate of temperature change of the first layer is equal to the rate of heat transfer from the second layer to the first layer minus the rate of heat transfer from the first layer to the tank wall. The equation is written as

$$\frac{\rho_1 Cp_1}{\Delta t}\left(\frac{A_0 + A_1}{2}\right)\Delta x_1 (T_1' - T_1)$$

$$= \frac{T_2 - T_1}{\Delta x_1/k_1[A_1 + (A_0 + A_1)/2] + \Delta x_2/k_2[A_1 + (A_1 + A_2)/2]}$$

$$- \frac{T_1 - T_0}{\Delta x_1/k_1[A_0 + (A_0 + A_1)/2]} \tag{18}$$

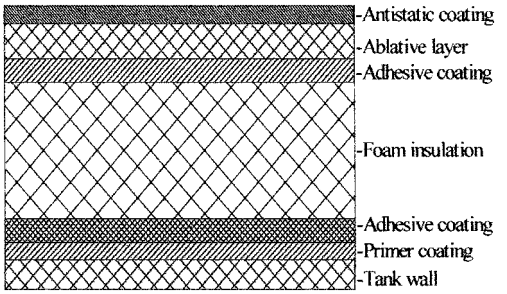

Fig. 3 Possible configuration of an integrated insulation package.

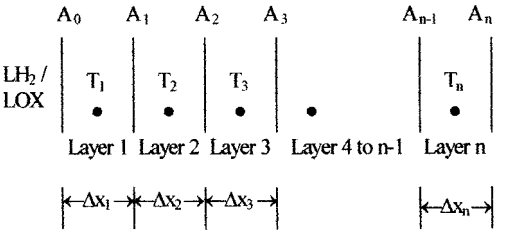

Fig. 4 Nomenclature of insulation layers for heat-transfer computations.

where subscripts 0 and 1 refer to the tank wall and layer number 1, respectively. The left-hand side of Eq. (18) represents the change of temperature (T_1', the new temperature) of the first layer after time interval Δt. The first term and the second term of the right-hand side compute the heat transfer from the second layer to the first layer and that from the first layer to the tank wall, respectively. Introducing for any ith layer,

$$B_i = \frac{\rho_i Cp_i}{\Delta t}\left(\frac{A_{i-1} + A_i}{2}\right)\Delta x_i$$

$$C_i = \left\{\frac{\Delta x_i}{k_i[A_i + (A_{i-1} + A_i)/2]} + \frac{\Delta x_{i+1}}{k_{i+1}[A_i + (A_i + A_{i+1})/2]}\right\}^{-1}$$

Equation(18) can be rearranged to obtain

$$T_1' = (1/B_1)[C_1 T_2 + C_0 T_0 - (C_0 - B_1 + C_1)T_1] \tag{19}$$

where

$$C_0 = \{\Delta x_1/k_1[A_0 + (A_0 + A_1)/2]\}^{-1}$$

Similarly for the second layer, heat equivalent to the rate of change of temperature is equal to the rate of heat transfer from the third layer to the second layer minus the rate of heat transfer from the second layer to the first layer. The equation is written as

$$\frac{\rho_2 Cp_2}{\Delta t}\left(\frac{A_1 + A_2}{2}\right)\Delta x_2 (T_2' - T_2)$$

$$= \frac{T_3 - T_2}{\Delta x_2/k_2[A_2 + (A_1 + A_2)/2] + \Delta x_3/k_3[A_2 + (A_2 + A_3)/2]}$$

$$- \frac{T_2 - T_1}{\Delta x_1/k_1[A_1 + (A_0 + A_1)/2] + \Delta x_2/k_2[A_1 + (A_1 + A_2)/2]} \tag{20}$$

or

$$T_2' = (1/B_2)[C_2 T_3 + C_1 T_1 - (C_1 - B_2 + C_2)T_2] \tag{21}$$

A similar set of equations can be written up to the $(n-1)$th layer. Thus the general equation form for any ith layer (for $1 \le i \le n-1$) is expressed as

$$T_i' = (1/B_i)[C_i T_{i+1} + C_{i-1} T_{i-1} - (C_{i-1} - B_i + C_i)T_i] \tag{22}$$

The outermost nth layer should take into account the conduction heat transfer $\dot{Q}_{\mathrm{COND}}$ from the nth layer to the $(n-1)$th layer in addition to the heat fluxes caused by $\dot{q}_{\mathrm{RADI}}$, $\dot{q}_{\mathrm{RADO}}$, and $\dot{q}_{\mathrm{CONV}}$ as defined in Eqs. (2), (16), and (17), respectively. The heat balance

after considering the heat fluxes just mentioned would enable the determination of the outer-layer temperature:

$$(\rho_n Cp_n/\Delta t)[(A_n + A_{n-1})/2]\Delta x_n(T'_n - T_n) = A_n(\dot{q}_{\text{RADI}} + \dot{q}_{\text{RADO}} + \dot{q}_{\text{CONV}}) - \dot{Q}_{\text{COND}} \quad (23)$$

Conduction heat transfer from the nth layer to the $(n-1)$th layer is estimated from

$$\dot{Q}_{\text{COND}} = \frac{(T_n - T_{n-1})}{\Delta x_{n-1}/k_{n-1}[A_{n-1} + (A_{n-2} + A_{n-1})/2] + \Delta x_n/k_n[A_{n-1} + (A_{n-1} + A_n)/2]} = C_{n-1}(T_n - T_{n-1}) \quad (24)$$

Using Eq. (24), Eq. (23) can be rearranged in the form of

$$T'_n = (1/B_n)[B_n T_n - C_{n-1}(T_n - T_{n-1}) + A_n(\dot{q}_{\text{RADI}} + \dot{q}_{\text{RADO}} + \dot{q}_{\text{CONV}})] \quad (25)$$

Thus at any instant when the temperatures of all of the layers are known, Eqs. (22) and (25) can be solved to generate a new set of temperatures for a given small time interval Δt. Temperatures of all of the layers at $t = 0$ are obtained from Eq. (1).

Stability, Accuracy, and Other Schemes

From the inherent characteristics of the finite difference simple explicit method, it can be shown[8–11] that the numerical solution of Eq. (22) is stable if and only if

$$B_i \geq C_{i-1} + C_i \qquad (\text{for } 1 \leq i \leq n-1) \quad (26)$$

A similar limitation in different form is also applicable to the outermost nth layer. If all of the layers are considered to be equal in width, area, and a single material with constant properties, then Eq. (26) reduces to $\Delta x^2/\beta\Delta t \geq 2$, which is the same as the stability limit for the one-dimensional unsteady conduction problem of a solid body with constant properties.[4]

Equation (22) has accuracy of the order $\mathcal{O}(\Delta t, \Delta x^2)$ indicating the significance of step sizes in time and space on the accuracy of the results. Thickness of some of the layers (adhesive, primer, etc.) in Fig. 3 are normally in the range of 100–150 μm, which are essentially the step sizes (Δx) indicated in Fig. 4. Using the lowest value of Δx, a limiting value of Δt can be obtained from Eq. (26). For example, in case of a liquid hydrogen tank insulated with foam, using a 100-μm step size, Δt is computed to be 0.006 s or lower. This involves a large number of iterations. However, with the availability of high-speed computers with high-precision data handling capability, computational time requirements can be insignificant, and sufficient accuracy can be achieved using this method.

It is possible to make the algorithm unconditionally stable if an implicit method is chosen instead of the explicit method as described earlier. In this method, Eqs. (18), (20), and (25) are modified to Eqs. (27–29), respectively:

$$B_1(T'_1 - T_1) = C_1(T'_2 - T'_1) - C_0(T'_1 - T_0) \quad (27)$$

$$B_i(T'_i - T_i) = C_i(T'_{i+1} - T'_i) - C_{i-1}(T'_i - T'_{i-1}) \qquad (\text{for } 2 \leq i \leq n-1) \quad (28)$$

$$B_n(T'_n - T_n) = \dot{Q}_{\text{INC}} - C_{n-1}(T'_n - T'_{n-1}) \quad (29)$$

where $\dot{Q}_{\text{INC}} = A_n(\dot{q}_{\text{RADI}} + \dot{q}_{\text{RADO}} + \dot{q}_{\text{CONV}})$. Thus n numbers of equations can be generated from Eqs. (27–29) for simultaneous solution of n numbers of unknown temperatures after a time interval Δt. These equations can be arranged in matrix form as shown next:

$$\begin{bmatrix} B_1 + C_1 + C_0 & -C_1 & & & & \\ -C_1 & B_2 + C_2 + C_1 & -C_2 & & 0 & \\ & -C_2 & B_3 + C_3 + C_2 & -C_3 & & \\ & & & & & \\ & 0 & & -C_{n-2} & B_{n-1} + C_{n-1} + C_{n-2} & -C_{n-1} \\ & & & & -C_{n-1} & B_n + C_{n-1} \end{bmatrix} \begin{bmatrix} T'_1 \\ T'_2 \\ T'_3 \\ \\ T'_{n-1} \\ T'_n \end{bmatrix} = \begin{bmatrix} B_1 T_1 + C_0 T_0 \\ B_2 T_2 \\ B_3 T_3 \\ \\ B_{n-1} T_{n-1} \\ B_n T_n + \dot{Q}_{\text{INC}} \end{bmatrix}$$

Standard procedures are available[8,10] for solving the preceding matrix form. The Gaussian elimination method was used by the author. This scheme also has the order of accuracy $\mathcal{O}(\Delta t, \Delta x^2)$. The advantage of this scheme over the explicit scheme is that considerably higher values of Δt (being unconditionally stable) can be used to reduce the number of iterations. To compare the results obtained from various solution methods, transient temperatures (at $t = 1000$ s) for selected locations in an insulation package are presented in Table 2. Insulation layer thickness for primer coating to antistatic coating (see Fig. 3) are 0.1, 0.4, 24.5, 0.4, 4.5, and 0.1 mm, respectively. Table 2 shows that compared to 0.006 s in the explicit method Δt in the implicit method can be taken as large as 5 s without any significant difference in temperature profile. However, the implicit scheme requires more computational effort.

The order of accuracy can be improved to $\mathcal{O}(\Delta t^2, \Delta x^2)$ if both explicit and implicit methods are combined using the Crank–Nicolson method.[8,10,11] The equivalent equations, for Eqs. (27–29), using this method, are expressed in Eqs. (30–32), respectively:

$$2B_1(T'_1 - T_1) = C_1(T'_2 - T'_1) - C_0(T'_1 - T_0) + C_1(T_2 - T_1) - C_0(T_1 - T_0) \quad (30)$$

$$2B_i(T'_i - T_i) = C_i(T'_{i+1} - T'_i) - C_{i-1}(T'_i - T'_{i-1}) + C_i(T_{i+1} - T_i) - C_{i-1}(T_i - T_{i-1}) \qquad (\text{for } 2 \leq i \leq n-1) \quad (31)$$

$$2B_n(T'_n - T_n) = 2\dot{Q}_{\text{INC}} - C_{n-1}(T'_n - T'_{n-1}) - C_{n-1}(T_n - T_{n-1}) \quad (32)$$

Table 2 Insulation temperatures (at t = 1000 s) at selected positions for various numerical schemes

	Temperature (K) at position from tank wall (mm):					
Scheme	0.05	5.09	11.22	17.34	23.47	29.34
Finite difference (explicit method) $\Delta t = 0.006$ s	21.74	119.68	183.87	231.56	271.54	305.67
Finite difference (implicit method) $\Delta t = 5.0$ s	21.74	119.68	183.87	231.56	271.53	305.66
Finite difference (Crank–Nicolson method) $\Delta t = 0.1$ s	21.74	119.68	183.87	231.56	271.54	305.67
Finite element (linear polynomial) $\Delta t = 0.006$ s	21.99	120.33	184.21	231.69	271.51	305.51
Finite element (quadratic polynomial) $\Delta t = 0.0007$ s	21.75	120.06	184.05	231.62	271.48	305.51

Similar to the implicit method, n numbers of equations can be generated from Eqs. (30–32) and organized in matrix form for solving simultaneously. This scheme, though unconditionally stable and of higher order accuracy, is known to produce considerable errors[11] for smaller values of $\Delta x^2/\beta\Delta t$. Hence, compared to the implicit method, Δt should be restricted to a lower value as indicated in Table 2. In spite of higher order of accuracy, there is no significant difference between the results of this method and that of the explicit or implicit method.

Comparison with Finite Element Solutions

Because an exact solution is not available, it is essential to verify the computed results with the solutions of other numerical methods. Galerkin finite element methods using linear and quadratic polynomial interpolants were considered, for which detailed formulations are derived in the Appendix. Results obtained from the finite element solutions are also presented in Table 2. As shown, there are minor differences between the finite difference and finite element solutions. Accuracy of the finite element analysis increases with higher-order polynomial interpolants.[12] This fact is reflected in Table 2, where the results of quadratic polynomial method are closer, compared to the results of linear method, to the finite difference solutions. However, the major disadvantages of using higher-order polynomial interpolants are lengthy derivations, large computer memory requirements, and very small Δt (0.0007 s, per Table 2) requirements for stability.

Sample Results and Discussions

To apply the numerical methods discussed, a computer program using C++ has been developed with options for various finite difference and finite element schemes. Sample results presented in this paper were obtained by the finite difference explicit method of solution. Computations were made based on the relevant information available for cryogenic rocket systems.[2,3] Results presented here are for a 2.8-m outer diameter (excluding insulation package) liquid hydrogen tank. All layers in the insulation package in Fig. 3 have been considered as rigid polyurethane foam. The thermal conductivity of foam is provided in the form of a third-order polynomial fit over the data available in literature.[13] The Srihorikota Range (SHAR) of India is considered as the launch site and is situated at about 13-deg north latitude. The date and local time of launch are taken as 20 January 2000 and 09:20 hrs, respectively. Ambient air temperature is taken as 300 K.

Transient temperature profiles across the insulation in section-I (see Fig. 1) are presented in Fig. 5. At $t = 0$ all of the insulation layers are seen to be at surface temperature computed from Eq. (1). Temperature profiles are shown in 30-s time intervals. Closely spaced temperature profiles indicate near steady-state heat transfer. Chill-down and filling of cryogenic rocket tanks normally require more than half an hour, indicating steady-state conditions after filling.

The outer surface temperature of insulation, under steady-state conditions, vs angular position (due south = 0, East +) is shown in Fig. 6. Constant temperature zones in the plot are the indication of no direct solar energy on the surface of that particular angular region. Similar characteristics are also observed in the heat flux variation shown in Fig. 7. Noticeable changes of heat flux in the presence of wind are indicated in Fig. 8. Significant reduction of heat fluxes, compared to still air, is expected if the surface temperature does not fall below the ambient air temperature. This trend may be reversed for small insulation thickness where the surface temperature may fall below ambient temperature and the wind velocity could cause an increase in heat in-leak. For example, in Fig. 6 (for 30-mm foam thickness) steady-state surface temperatures drop below room temperature in the angular region of 138 to 318 deg. In this angular region, heat fluxes increase as shown in Fig. 8.

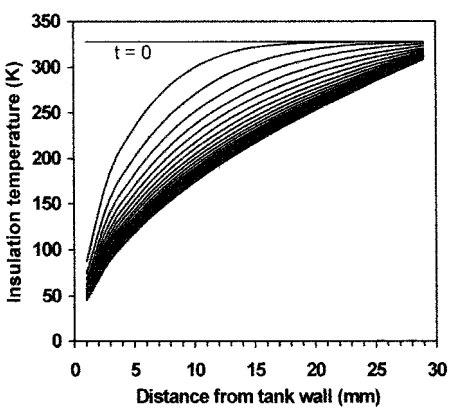

Fig. 5 Transient temperature profiles, with 30-s time interval, for section-I of LH_2 tank insulation (wind velocity = 0).

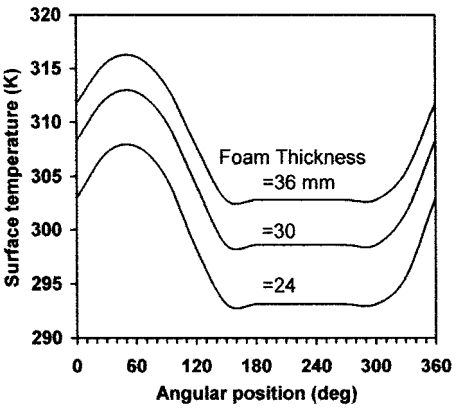

Fig. 6 Insulation surface temperature in angular direction under steady-state condition (wind velocity = 0).

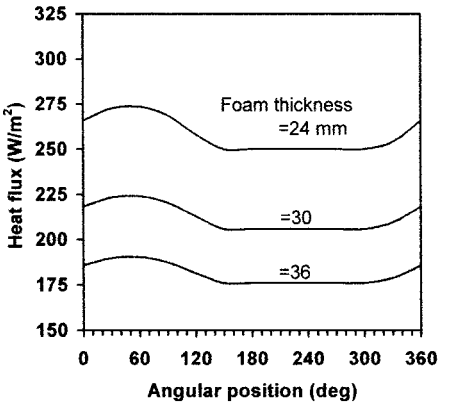

Fig. 7 Heat in-leak in angular direction under steady-state condition (wind velocity = 0).

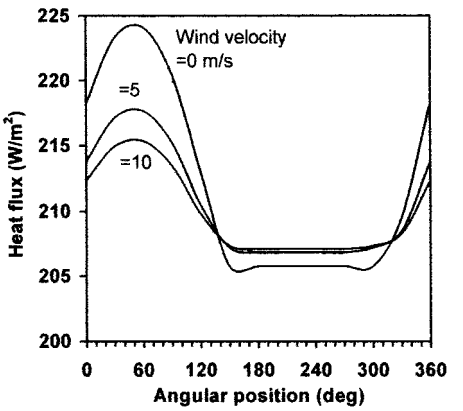

Fig. 8 Heat in-leak (steady state) in angular direction as function of wind velocity (foam thickness = 30 mm, wind flow from southeast).

Conclusions

This paper presents a theoretical model for predicting the thermal performance of insulating materials for cryogenic rocket propellant tanks. The model considers only the cylindrical sides of the propellant tanks during ground-hold conditions. Estimation of solar radiation, Earth-reflected/emitted radiation, and heat exchange with the surrounding air are included.

A finite difference technique using the simple explicit scheme is adopted for computing temperature distributions under transient conditions. A stability analysis of the scheme indicates the requirement for a large number of iterations. A simple implicit scheme could reduce the number of iterations significantly with increased computer programing effort. The Crank–Nicolson scheme is found to be slightly advantageous over the simple implicit scheme. The results of the finite difference schemes were verified with Galerkin finite element solutions using linear and quadratic polynomial interpolants. Good matching was observed with the quadratic polynomial results. Sample results have been presented based on relevant input data. The model should be useful to space engineers in design selection and performance prediction of cryogenic rocket stage insulation systems.

Appendix: Galerkin Finite Element Methods

Linear Polynomial Interpolants

Shih[12] describes the detailed developmental procedure in Galerkin finite element methods. Using the one-dimensional transient heat-transfer equation[8] in the cylindrical coordinate system, one has

$$\frac{1}{x}\frac{\partial}{\partial x}\left(kx\frac{\partial T}{\partial x}\right)=\rho Cp\frac{\partial T}{\partial t} \tag{A1}$$

or

$$\frac{\partial^2 T}{\partial x^2}+\left(\frac{1}{x}+\frac{1}{k}\frac{\partial k}{\partial x}\right)\frac{\partial T}{\partial x}=\frac{1}{\beta}\frac{\partial T}{\partial t} \tag{A2}$$

Considering each layer to be a finite element as shown in Fig. A1, the general form of temperature approximation used in this method is given by

$$\tilde{T}(x)=\sum_{j=0}^{n} T_j N_j(x)$$

Construction of piecewise linear basis functions $N_j(x)$, their local support and corresponding temperature functions are described in Fig. A2. The values of N_j anywhere outside the domain $[x_{j-1}, x_{j+1}]$ are zero. Using the Galerkin approach, Eq. (A2) is multiplied by the weighting functions N_j (same as the basis functions) and then integrated over the total width of insulation package. Mathematically it is expressed as

$$-\int_{x_0}^{x_n} N_j\frac{\mathrm{d}^2\tilde{T}}{\mathrm{d}x^2}\,\mathrm{d}x-\int_{x_0}^{x_n}\frac{N_j}{x}\frac{\mathrm{d}\tilde{T}}{\mathrm{d}x}\,\mathrm{d}x-\int_{x_0}^{x_n}\frac{N_j}{k}\frac{\mathrm{d}k}{\mathrm{d}x}\frac{\mathrm{d}\tilde{T}}{\mathrm{d}x}\,\mathrm{d}x+\int_{x_0}^{x_n}\frac{N_j}{\beta}\frac{\mathrm{d}\tilde{T}}{\mathrm{d}t}\mathrm{d}x=0 \tag{A3}$$

Using $j=1$ to n in Eq. (A3), it is possible to generate n numbers of equations that need to be solved simultaneously. Applying integration by parts to the first integral of Eq. (A3), one gets

$$\int_{x_0}^{x_n}\frac{\mathrm{d}\tilde{T}}{\mathrm{d}x}\frac{\mathrm{d}N_j}{\mathrm{d}x}\,\mathrm{d}x-N_j\frac{\mathrm{d}\tilde{T}}{\mathrm{d}x}\bigg|_{x_0}^{x_n}-\int_{x_0}^{x_n}\frac{N_j}{x}\frac{\mathrm{d}\tilde{T}}{\mathrm{d}x}\,\mathrm{d}x-\int_{x_0}^{x_n}\frac{N_j}{k}\frac{\mathrm{d}k}{\mathrm{d}x}\frac{\mathrm{d}\tilde{T}}{\mathrm{d}x}\,\mathrm{d}x+\int_{x_0}^{x_n}\frac{N_j}{\beta}\frac{\mathrm{d}\tilde{T}}{\mathrm{d}t}\,\mathrm{d}x=0 \tag{A4}$$

From the definition of N_j for $1\le j\le n-1$, N_j is zero both at $x=x_0$ and $x=x_n$. Thus Eq. (A4) is expressed in the form

$$\int_{x_{j-1}}^{x_{j+1}}\frac{\mathrm{d}\tilde{T}}{\mathrm{d}x}\frac{\mathrm{d}N_j}{\mathrm{d}x}\,\mathrm{d}x-\int_{x_{j-1}}^{x_{j+1}}\frac{N_j}{x}\frac{\mathrm{d}\tilde{T}}{\mathrm{d}x}\,\mathrm{d}x-\int_{x_{j-1}}^{x_{j+1}}\frac{N_j}{k}\frac{\mathrm{d}k}{\mathrm{d}x}\frac{\mathrm{d}\tilde{T}}{\mathrm{d}x}\,\mathrm{d}x+\int_{x_{j-1}}^{x_{j+1}}\frac{N_j}{\beta}\frac{\mathrm{d}\tilde{T}}{\mathrm{d}t}\,\mathrm{d}x=0 \tag{A5}$$

An average value of thermal conductivity, for the elements $[x_{j-1}, x_j]$, is adopted as $k_{j-1,j}=0.5\,(k_{j-1}+k_j)$. A similar approach is also used to estimate average Cp values. The slope of thermal conductivity is computed from

$$\left(\frac{\mathrm{d}k}{\mathrm{d}x}\right)_{j-1,j}=\frac{k_j-k_{j-1}}{\Delta x_{j-1,j}}\qquad(\text{for } j=1 \text{ and } n)$$

and[12]

$$\left(\frac{\mathrm{d}k}{\mathrm{d}x}\right)_{j-1,j}=\frac{k_{j,j+1}+k_{j-1,j}(\lambda^2-1)-\lambda^2 k_{j-2,j-1}}{0.5(\Delta x_{j-1,j}+\Delta x_{j,j+1})(1+\lambda)}$$

$$(\text{for } 2\le j\le n-1) \tag{A6}$$

where

$$\lambda=\frac{\Delta x_{j-1,j}+\Delta x_{j,j+1}}{\Delta x_{j-2,j-1}+\Delta x_{j-1,j}}$$

With these data and the information given in Fig. A2, Eq. (A5) is integrated to obtain

$$\begin{aligned}&\frac{\mathrm{d}T_{j-1}}{\mathrm{d}t}\left(\frac{\Delta x}{6\beta}\right)_{j-1,j}+\frac{\mathrm{d}T_j}{\mathrm{d}t}\left[\left(\frac{\Delta x}{3\beta}\right)_{j-1,j}+\left(\frac{\Delta x}{3\beta}\right)_{j,j+1}\right]\\&+\frac{\mathrm{d}T_{j+1}}{\mathrm{d}t}\left(\frac{\Delta x}{6\beta}\right)_{j,j+1}+T_{j-1}\left[\frac{-x_{j-1}}{\Delta x_{j-1,j}^2}\ell_n\left(\frac{x_j}{x_{j-1}}\right)\right.\\&\left.+\frac{1}{2}\left(\frac{1}{k}\frac{\mathrm{d}k}{\mathrm{d}x}\right)_{j-1,j}\right]+T_j\left[\frac{x_{j-1}}{\Delta x_{j-1,j}^2}\ell_n\left(\frac{x_j}{x_{j-1}}\right)\right.\\&\left.+\frac{x_{j+1}}{\Delta x_{j,j+1}^2}\ell_n\left(\frac{x_{j+1}}{x_j}\right)-\frac{1}{2}\left(\frac{1}{k}\frac{\mathrm{d}k}{\mathrm{d}x}\right)_{j-1,j}+\frac{1}{2}\left(\frac{1}{k}\frac{\mathrm{d}k}{\mathrm{d}x}\right)_{j,j+1}\right]\\&+T_{j+1}\left[\frac{-x_{j+1}}{\Delta x_{j,j+1}^2}\ell_n\left(\frac{x_{j+1}}{x_j}\right)-\frac{1}{2}\left(\frac{1}{k}\frac{\mathrm{d}k}{\mathrm{d}x}\right)_{j,j+1}\right]=0\end{aligned}$$

$$(\text{for } 1\le j\le n-1) \tag{A7}$$

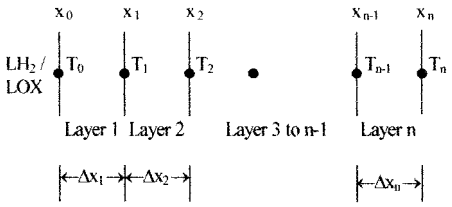

Fig. A1 Node distribution for finite element method using linear interpolants.

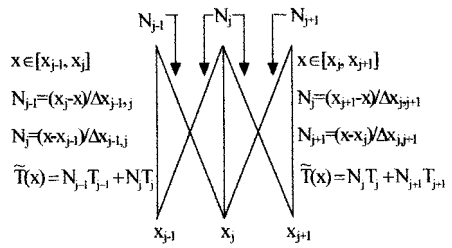

Fig. A2 Construction of piecewise linear basis functions and temperature approximations.

From the boundary condition at $x = x_0$, we have, for $j = 1$ and $t \geq 0$, T_{j-1} = propellant temperature and $\mathrm{d}T_{j-1}/\mathrm{d}t = 0$. The boundary condition for $j = n$ can be expressed as

$$k_{n-1,n}\left(\frac{\mathrm{d}T}{\mathrm{d}x}\right)_{x=x_n} = \dot{q}_{\mathrm{RADI}} + \dot{q}_{\mathrm{RADO}} + \dot{q}_{\mathrm{CONV}} = \dot{q}_{\mathrm{INC}} \tag{A8}$$

The boundary condition term in Eq. (A4) does not vanish for $j = n$, and it is evaluated as[12]

$$N_n \frac{\mathrm{d}T}{\mathrm{d}x}\bigg|_{x_0}^{x_n} = N_n(x_n)\left(\frac{\mathrm{d}T}{\mathrm{d}x}\right)_{x=x_n} - N_n(x_0)\left(\frac{\mathrm{d}T}{\mathrm{d}x}\right)_{x=x_0}$$

$$= \left(\frac{\mathrm{d}T}{\mathrm{d}x}\right)_{x=x_n} = \frac{\dot{q}_{\mathrm{INC}}}{k_{n-1,n}} \tag{A9}$$

Using Eq. (A9) in Eq. (A4) and carrying out the necessary integration (for $j = n$), one gets

$$\frac{\mathrm{d}T_{n-1}}{\mathrm{d}t}\left(\frac{\Delta x}{6\beta}\right)_{n-1,n} + \frac{\mathrm{d}T_n}{\mathrm{d}t}\left(\frac{\Delta x}{3\beta}\right)_{n-1,n} + T_{n-1}\left[\frac{-x_{n-1}}{\Delta x^2_{n-1,n}} \times \ell_n\left(\frac{x_n}{x_{n-1}}\right) + \frac{1}{2}\left(\frac{1}{k}\frac{\mathrm{d}k}{\mathrm{d}x}\right)_{n-1,n}\right] + T_n\left[\frac{x_{n-1}}{\Delta x^2_{n-1,n}} \times \ell_n\left(\frac{x_n}{x_{n-1}}\right) - \frac{1}{2}\left(\frac{1}{k}\frac{\mathrm{d}k}{\mathrm{d}x}\right)_{n-1,n}\right] - \frac{\dot{q}_{\mathrm{INC}}}{k_{n-1,n}} = 0 \tag{A10}$$

Equations (A7) and (A10) constitute a set of linear first-order ordinary differential equations. Starting from all known temperatures at $t = 0$, we solve $\mathrm{d}T_j/\mathrm{d}t$, for $j = 1, 2, \ldots, n$, and then considering a small time interval, the new temperatures are obtained. Similarly, computations for any time step are performed based on the temperatures obtained in the preceding time step. The intermediate temperatures, at any location, can be obtained from the relations given in Fig. A2. Thus solutions are obtained continuously in space and discretely with time.

Quadratic Polynomial Interpolants

In a quadratic system an additional node point at the middle of the two endpoints of the elements is used.[12] Thus for n number of elements, one has a total $2n + 1$ number nodes in which the temperature of the starting node ($j = 0$) is always known T_0, indicating $2n$ numbers of unknown temperatures to be determined. In this method the weighting functions for $j = 1, 3, 5, \ldots, 2(n-1)$, have support on the element $[x_{j-1}, x_{j+1}]$, whereas for $j = 2, 4, 6, \ldots, 2(n-1)$ these have support on two elements $[x_{j-2}, x_j]$ and $[x_j, x_{j+2}]$ with x_j being the position of elemental interface. Therefore the formulation will be presented for odd and even j separately.

For $j = 1, 3, 5, \ldots, 2(n-1)$ the temperatures at the positions x_{j-1}, x_j, and x_{j+1} are identified as T_{j-1}, T_j, and T_{j+1}, respectively. Applying these spatial temperature conditions in a quadratic polynomial interpolation function, the temperature approximation can be expressed in the form

$$\tilde{T}(x) = W_{j-1}(x)T_{j-1} + W_j(x)T_j + W_{j+1}(x)T_{j+1} \tag{A11}$$

where the basis functions are defined as [using $X = (x - x_{j-1})/(x_{j+1} - x_{j-1}) = (x - x_{j-1})/\Delta x_{j-1,j+1}$]

$$W_{j-1}(x) = 1 - 3X + 2X^2 \tag{A12}$$

$$W_j(x) = 4(X - X^2) \tag{A13}$$

$$W_{j+1}(x) = 2X^2 - X \tag{A14}$$

In Eq. (A3) replacing N_j with W_j and applying integration parts to the first integral, we obtain the equation similar to Eq. (A5) as

$$\int_{x_{j-1}}^{x_{j+1}} \frac{\mathrm{d}W_j}{\mathrm{d}x}\frac{\mathrm{d}\tilde{T}}{\mathrm{d}x}\,\mathrm{d}x - \int_{x_{j-1}}^{x_{j+1}} \frac{W_j}{x}\frac{\mathrm{d}\tilde{T}}{\mathrm{d}x}\,\mathrm{d}x - \int_{x_{j-1}}^{x_{j+1}} \frac{W_j}{k}\frac{\mathrm{d}k}{\mathrm{d}x}\frac{\mathrm{d}\tilde{T}}{\mathrm{d}x}\,\mathrm{d}x + \int_{x_{j-1}}^{x_{j+1}} \frac{W_j}{\beta}\frac{\mathrm{d}\tilde{T}}{\mathrm{d}t}\,\mathrm{d}x = 0 \tag{A15}$$

Using the relations given in Eq. (A11–A14), Eq. (A15) is integrated to obtain

$$\frac{\mathrm{d}T_{j-1}}{\mathrm{d}t}\left(\frac{\Delta x}{15\beta}\right)_{j-1,j+1} + \frac{\mathrm{d}T_j}{\mathrm{d}t}\left(\frac{8\Delta x}{15\beta}\right)_{j-1,j+1} + \frac{\mathrm{d}T_{j+1}}{\mathrm{d}t}\left(\frac{\Delta x}{15\beta}\right)_{j-1,j+1}$$

$$+ T_{j-1}\left[\frac{2}{3\Delta x} + \frac{20x_{j-1}}{\Delta x^2} + \frac{16x^2_{j-1}}{\Delta x^3} - \ell_n\left(\frac{x_{j+1}}{x_{j-1}}\right) \times \left(\frac{16x^3_{j-1}}{\Delta x^4} + \frac{28x^2_{j-1}}{\Delta x^3} + \frac{12x_{j-1}}{\Delta x^2}\right) + \frac{2}{3k}\frac{\mathrm{d}k}{\mathrm{d}x}\right]_{j-1,j+1}$$

$$+ T_j\left[\frac{8}{3\Delta x} - \frac{32x_{j-1}}{\Delta x^2} + \frac{32x^2_{j-1}}{\Delta x^3} + \ell_n\left(\frac{x_{j+1}}{x_{j-1}}\right) \times \left(\frac{32x^3_{j-1}}{\Delta x^4} + \frac{48x^2_{j-1}}{\Delta x^3} + \frac{16x_{j-1}}{\Delta x^2}\right)\right]_{j-1,j+1}$$

$$+ T_{j+1}\left[\frac{-10}{3\Delta x} + \frac{12x_{j-1}}{\Delta x^2} + \frac{16x^2_{j-1}}{\Delta x^3} - \ell_n\left(\frac{x_{j+1}}{x_{j-1}}\right) \times \left(\frac{16x^3_{j-1}}{\Delta x^4} + \frac{20x^2_{j-1}}{\Delta x^3} + \frac{4x_{j-1}}{\Delta x^2}\right) - \frac{2}{3k}\frac{\mathrm{d}k}{\mathrm{d}x}\right]_{j-1,j+1} = 0$$

$$(\text{for } j = 1, 3, 5, \ldots, 2n-1) \tag{A16}$$

For $j = 2, 4, 6, \ldots, 2(n-1)$ we change the integration limit in Eq. (A15) and rewrite

$$\int_{x_{j-2}}^{x_{j+2}} \frac{\mathrm{d}W_j}{\mathrm{d}x}\frac{\mathrm{d}\tilde{T}}{\mathrm{d}x}\,\mathrm{d}x - \int_{x_{j-2}}^{x_{j+2}} \frac{W_j}{x}\frac{\mathrm{d}\tilde{T}}{\mathrm{d}x}\,\mathrm{d}x - \int_{x_{j-2}}^{x_{j+2}} \frac{W_j}{k}\frac{\mathrm{d}k}{\mathrm{d}x}\frac{\mathrm{d}\tilde{T}}{\mathrm{d}x}\,\mathrm{d}x + \int_{x_{j-2}}^{x_{j+2}} \frac{W_j}{\beta}\frac{\mathrm{d}\tilde{T}}{\mathrm{d}t}\,\mathrm{d}x = 0 \tag{A17}$$

The basis functions and temperature approximations are reframed as

$$W_{j-2}(x) = W_j^+(x) = 1 - 3X + 2X^2 \tag{A18}$$

$$W_{j-1}(x) = W_{j+1}(x) = 4(X - X^2) \tag{A19}$$

$$W_j^-(x) = W_{j+2}(x) = 2X^2 - X \tag{A20}$$

where, for $x \in [x_{j-2}, x_j]$,

$$X = \frac{x - x_{j-2}}{x_j - x_{j-2}} = \frac{x - x_{j-2}}{\Delta x_{j-2,j}} \tag{A21}$$

$$\tilde{T}(x) = W_{j-2}(x)T_{j-2} + W_{j-1}(x)T_{j-1} + W_j^-(x)T_j \tag{A22}$$

and, for $x \in [x_j, x_{j+2}]$,

$$X = \frac{x - x_j}{x_{j+2} - x_j} = \frac{x - x_j}{\Delta x_{j,j+2}} \tag{A23}$$

$$\tilde{T}(x) = W_j^+(x)T_j + W_{j+1}(x)T_{j+1} + W_{j+2}(x)T_{j+2} \tag{A24}$$

Using Eqs. (A18–A24), Eq. (A17) can be integrated to obtain

$$\frac{dT_{j-2}}{dt}\left(\frac{-\Delta x}{30\beta}\right)_{j-2,j}+\frac{dT_{j-1}}{dt}\left(\frac{\Delta x}{15\beta}\right)_{j-2,j}+\frac{dT_j}{dt}\left(\frac{2\Delta x}{15\beta_{j-2,j}}+\frac{2\Delta x}{15\beta_{j,j+2}}\right)+\frac{dT_{j+1}}{dt}\left(\frac{\Delta x}{15\beta}\right)_{j,j+2}+\frac{dT_{j+2}}{dt}\left(\frac{-\Delta x}{30\beta}\right)_{j,j+2}$$
$$+T_{j-2}\left[\frac{-1}{3\Delta x}-\frac{6x_{j-2}}{\Delta x^2}-\frac{8x_{j-2}^2}{\Delta x^3}+\ell n\left(\frac{x_j}{x_{j-2}}\right)\left(\frac{8x_{j-2}^3}{\Delta x^4}+\frac{10x_{j-2}^2}{\Delta x^3}+\frac{3x_{j-2}}{\Delta x^2}\right)-\frac{1}{6k}\frac{dk}{dx}\right]_{j-2,j}+T_{j-1}\left[\frac{-4}{3\Delta x}+\frac{8x_{j-2}}{\Delta x^2}+\frac{16x_{j-2}^2}{\Delta x^3}-\ell n\left(\frac{x_j}{x_{j-2}}\right)\left(\frac{16x_{j-2}^3}{\Delta x^4}+\frac{16x_{j-2}^2}{\Delta x^3}+\frac{4x_{j-2}}{\Delta x^2}\right)+\frac{2}{3k}\frac{dk}{dx}\right]_{j-2,j}$$
$$+T_j\left\{\left[\frac{5}{3\Delta x}-\frac{2x_{j-2}}{\Delta x^2}-\frac{8x_{j-2}^2}{\Delta x^3}+\ell n\left(\frac{x_j}{x_{j-2}}\right)\left(\frac{8x_{j+2}^3}{\Delta x^4}+\frac{6x_{j-2}^2}{\Delta x^3}+\frac{x_{j-2}}{\Delta x^2}\right)-\frac{1}{2k}\frac{dk}{dx}\right]_{j-2,j}-\left[\frac{13}{3\Delta x}+\frac{14x_j}{\Delta x^2}+\frac{8x_j^2}{\Delta x^3}-\ell n\left(\frac{x_{j+2}}{x_j}\right)\left(\frac{8x_j^3}{\Delta x^4}+\frac{18x_j^2}{\Delta x^3}+\frac{13x_j}{\Delta x^2}+\frac{3}{\Delta x}\right)-\frac{1}{2k}\frac{dk}{dx}\right]_{j,j+2}\right\}+T_{j+1}\left[\frac{20}{3\Delta x}+\frac{24x_j}{\Delta x^2}+\frac{16x_j^2}{\Delta x^3}-\ell n\left(\frac{x_{j+2}}{x_j}\right)\left(\frac{16x_j^3}{\Delta x^4}+\frac{32x_j^2}{\Delta x^3}+\frac{20x_j}{\Delta x^2}+\frac{4}{\Delta x}\right)-\frac{2}{3k}\frac{dk}{dx}\right]_{j,j+2}+T_{j+2}\left[\frac{-7}{3\Delta x}-\frac{10x_j}{\Delta x^2}-\frac{8x_j^2}{\Delta x^3}+\ell n\left(\frac{x_{j+2}}{x_j}\right)\times\left(\frac{8x_j^3}{\Delta x^4}+\frac{14x_j^2}{\Delta x^3}+\frac{7x_j}{\Delta x^2}+\frac{1}{\Delta x}\right)+\frac{1}{6k}\frac{dk}{dx}\right]_{j,j+2}=0 \quad \text{(A25)}$$

At the outermost surface the boundary condition term should be included in Eq. (A17), and following the similar procedure used to develop Eqs. (A8–A10), the equation for the last node is obtained as (for $j=2n$)

$$\left[\frac{dT_{2n-2}}{dt}\left(\frac{-\Delta x}{30\beta}\right)+\frac{dT_{2n-1}}{dt}\left(\frac{\Delta x}{15\beta}\right)+\frac{dT_{2n}}{dt}\left(\frac{2\Delta x}{15\beta}\right)\right]_{2n-2,2n}$$
$$+T_{2n-2}\left[\frac{-1}{3\Delta x}-\frac{6x_{2n-2}}{\Delta x^2}-\frac{8x_{2n-2}^2}{\Delta x^3}+\ell n\left(\frac{x_{2n}}{x_{2n-2}}\right)\times\left(\frac{8x_{2n-2}^3}{\Delta x^4}+\frac{10x_{2n-2}^2}{\Delta x^3}+\frac{3x_{2n-2}}{\Delta x^2}\right)-\frac{1}{6k}\frac{dk}{dx}\right]_{2n-2,2n}$$
$$+T_{2n-1}\left[\frac{-4}{3\Delta x}+\frac{8x_{2n-2}}{\Delta x^2}+\frac{16x_{2n-2}^2}{\Delta x^3}-\ell n\left(\frac{x_{2n}}{x_{2n-2}}\right)\times\left(\frac{16x_{2n-2}^3}{\Delta x^4}+\frac{16x_{2n-2}^2}{\Delta x^3}+\frac{4x_{2n-2}}{\Delta x^2}\right)+\frac{2}{3k}\frac{dk}{dx}\right]_{2n-2,2n}$$
$$+T_{2n}\left[\frac{5}{3\Delta x}-\frac{2x_{2n-2}}{\Delta x^2}-\frac{8x_{2n-2}^2}{\Delta x^3}+\ell n\left(\frac{x_{2n}}{x_{2n-2}}\right)\times\left(\frac{8x_{2n-2}^3}{\Delta x^4}+\frac{6x_{2n-2}^2}{\Delta x^3}+\frac{x_{2n-2}}{\Delta x^2}\right)-\frac{1}{2k}\frac{dk}{dx}\right]_{2n-2,2n}-\frac{\dot{q}_{\text{INC}}}{k_{2n-2,2n}}=0 \quad \text{(A26)}$$

Thus Eqs. (A16), (A18), and (A19) generate n, $n-1$, and 1 numbers of equations, respectively, which in aggregate make $2n$ numbers of equations for $2n$ numbers of unknown temperatures. The procedure for simultaneous solution of these equations is the same as that used for linear polynomial case. The thermal conductivity and Cp values are computed with respect to the temperature at the middle node of the elements, and the change of thermal conductivity with respect to x are determined using the equivalent form of Eq. (A6).

Acknowledgments

The author thankfully acknowledges the support given by the Liquid Propulsion Systems Centre, Indian Space Research Organisation, Valiamala, Thiruvananthapuram, and the Indian Institute of Technology, Kharagpur, for conducting the effort.

References

[1]McGrew, J. L., "A Comparative Study of Airborne Liquid-Hydrogen Tank Insulation," *Advances in Cryogenic Engineering*, Vol. 8, edited by K. D. Timmerhaus, Plenum, New York, 1963, pp. 387–392.

[2]Menard, J., and Triol, J., "Structural Cryogenic Vessels of Rocket Stages," *Liquid Hydrogen: Properties, Production and Application*, Paris, 1965, pp. 159–180.

[3]Huzel, D. K., and Huang, D. H., "Design of Liquid Propellant Rocket Engines," 2nd ed. NASA SP-125, 1971.

[4]Holman, J. P., *Heat Transfer*, 6th ed., McGraw–Hill, London, 1986, pp. 131–206, 271–372, 459–470.

[5]Bayazitoglu, Y., "Availability of Solar Energy," *Solar Energy Utilization* edited by H. Yuncu, E. Paykoc, and Y. Yener, Martinus–Nijhoff, Dordrecht, The Netherlands, 1987, pp. 45–68.

[6]Siegel, R., and Howell, J. R., *Thermal Radiation Heat Transfer (Solutions Manual)*, 3rd ed., Taylor and Francis, Bristol, England, U.K., 1993, pp. 6.17, 6.18.

[7]Zukauskas, A., and Ziugzda, J., *Heat Transfer of a Cylinder in Crossflow*, Hemisphere, Washington, DC, 1985, pp. 97–127.

[8]Özisik, M. N., *Heat Conduction*, 2nd ed., Wiley, New York, 1993, pp. 3–9, 436–501.

[9]Anderson, D. A., Tanehill, J. C., and Pletcher, R. H., *Computational Fluid Mechanics and Heat Transfer*, Hemisphere, New York, 1984, pp. 108,109.

[10]Mathews, J. H., *Numerical Methods*, 2nd ed., Prentice–Hall of India, New Delhi, India, 1994, pp. 509–519.

[11]Krishnamurthy, E. V., and Sen, S. K., *Numerical Algorithms*, 2nd ed., Affiliated East-West Press Pvt., Ltd., New Delhi, India, 1986, pp. 445, 446, 560, 561.

[12]Shih, T. M., *Numerical Heat Transfer*, Hemisphere, New York, 1984, pp. 14–27, 84–88, 521–522, 538.

[13]Bock, R., and Zollner, R., "Polyurethane Rigid Foam," *Polyurethane Handbook*, 2nd ed., edited by G. Oertel, Carl Hanser Verlag, New York, 1994, pp. 271–274.

M. Torres
Associate Editor